International Journal of Thermal Sciences 49 (2010) 153–160

Contents lists available at ScienceDirect

International Journal of Thermal Sciences

journal homepage: www.elsevier.com/locate/ijts

Slip flow heat transfer in an infinite microtube with axial conduction

Ashok K. Satapathy*

Department of Mechanical Engineering, National Institute of Technology, Rourkela-769 008, Orissa, India

ARTICLE INFO

Article history:
Received 29 April 2009
Received in revised form
26 June 2009
Accepted 30 June 2009
Available online 24 July 2009

Keywords:
Microscale
Heat transfer
Slip-flow
Slug-flow
Analytical solution

ABSTRACT

This paper deals with analytical solution of steady-state heat transfer for laminar, two-dimensional and rarefied gas flow in an infinite microtube subjected to mixed boundary conditions. To account for the slip-flow characteristics of microscale heat transfer, temperature jump condition at the wall has been incorporated in the model while the fluid velocity is assumed to be constant (slug flow). The energy equation in the thermal entrance region has been solved by the method of separation of variables. The solution yields closed form expressions for bulk-mean temperature and Nusselt number in terms of Knudsen number and Peclet number.

1. Introduction

The trend of miniaturization of electronic systems requires effective cooling from a relatively small surface area and thus requires efficient thermal control methods. Devices having dimensions of the order of micrometers are being developed for cooling of integrated circuits, biochemical applications, micro-electromechanical systems and optoelectronics. Hence, the development of efficient cooling techniques associated with microelectronic devices is one of the important contemporary applications of microscale heat transfer. This imperative requirement has initiated an extensive research in microchannel/microtube cooling. A number of analytic solutions have been reported in the literature for predicting the flow and temperature of the coolant, which is essential for thermal design of microdevices.

In case of gaseous flow in a microtube or microchannel, the mean free path of gas molecules becomes comparable to the characteristic length of the system. Under such circumstances, the no-slip boundary conditions become no longer valid so that velocity slip and temperature jump conditions on the wall need to be considered. The incorporation of slip boundary condition is also essential if the fluid is at low pressure. The rarefaction effect of gas is generally represented by Knudsen number, Kn, which is defined as the ratio of molecular mean free path to characteristic length of the flow geometry. Continuum equations are applicable for $Kn \to 0$, while kinetic theory is valid for $Kn \to \infty$ (free molecular flow). The flow regime, in which the Knudsen number ranges from 10^{-3} to 10^{-1}, is termed as "slip-flow". Since the slip-flow regime nearly behaves as that of a continuum regime, the heat transfer phenomena in the slip-flow regime can be safely modeled using continuum equations together with slip-flow boundary conditions [1].

In a conventional Graetz problem the flow is considered to be hydrodynamically fully developed but thermally developing and, viscous dissipation and axial conduction are neglected. Also, the fully-developed velocity profile used in the energy equation is considered to be parabolic. The Graetz problem has subsequently been extended by many investigators so as to include axial conduction and viscous dissipation in tube/channel geometries. The extended Graetz problem in the slip-flow regime has also been investigated by several researchers in microchannels [2–7] and in microtubes [8–14]. The analytical methods commonly adopted are separation of variables, integral transform technique and direct simulation Monte-Carlo (DSMC) technique.

Using the method of separation of variables, the effect of axial conduction together with viscous dissipation for thermally developing flow was studied by Jeong and Jeong [2] in a microchannel and by Jeong and Jeong [12] in a microtube. Hadjiconstantinou and Simek [3] solved the constant-wall-temperature heat transfer characteristics of a model gaseous flow in micro and nano channels by the DSMC technique. Yu and Ameel [4] applied a modified generalized integral transform technique to solve the energy

* Tel.: +91 661 2462522; fax: +91 661 2472926.
E-mail addresses: aksatapathy2010@gmail.com, aksatapathy2003@rediff.com

1290-0729/$ – see front matter © 2009 Elsevier Masson SAS. All rights reserved.
doi:10.1016/j.ijthermalsci.2009.06.012

Nomenclature

c_p	specific heat
D_h	hydraulic diameter, $D_h = 2R_0$
F_t	thermal accommodation coefficient
h	heat transfer coefficient
J_0, J_1	Bessel functions
k	thermal conductivity
Kn	Knudsen number, $Kn = \lambda/D_h$
Nu	Nusselt number, $Nu = hD_h/k$
Pe	Peclet number, $Pe = \rho c_p U R_0/k$
Pr	Prandtl number, $Pr = \mu c_p/k$
R_0	radius of the tube
s	half of Peclet number, $s = Pe/2$
T	temperature
U	constant fluid velocity
R,Z	physical coordinates
r, z	dimensionless coordinates
β	eigen values
γ	specific heat ratio
λ	molecular mean free path, eigen values
μ	dynamic viscosity
ρ	density
θ	dimensionless temperature, $\theta = (T - T_w)/(T_0 - T_w)$

Subscripts

0	inlet condition
A	isothermal zone
B	adiabatic zone
b	bulk-mean values
w	wall condition
∞	fully-developed

equation for the slip-flow regime in a rectangular microchannel. Tunc and Bayazitoglu studied the slip-flow heat transfer in microchannels [5] and in microtubes [11] for both uniform temperature and uniform heat flux boundary conditions, by the use of the integral transform technique. The effects of rarefaction and surface accommodation coefficient on slip-flow heat transfer were studied by Chen [6] for a microchannel and by Larrode et al. [10] for a microtube. Aydin and Avci obtained an analytical solution to laminar forced convection in a microchannel [7] and in a microtube [13,14] for the slip-flow regime under constant wall temperature and constant wall heat flux boundary conditions, considering the viscous dissipation effect. Barron et al. [8] extended the Graetz problem to slip-flow regime for constant wall temperature condition and solved the energy equation by power series method. Ameel et al. [9] also employed similar solution method to solve the problem of gaseous slip-flow in microtubes with constant heat flux boundary condition.

In the slug flow model, it is assumed that the velocity of the fluid is uniform across any cross-section of the tube perpendicular to the axis of the tube and there is no boundary layer adjacent to the inner wall of the pipe. The slug flow heat transfer problem in a semi-infinite tube was solved by Golos [15] by the use of Laplace transformation assuming a constant heat transfer coefficient. Using Laplace transform method and Galerkin's technique, the above problem was also solved by Tyagi and Nigam [16]. The slug flow forced convection with viscous dissipation was studied by Barletta and Zanchini [17] assuming constant heat transfer coefficient and by Barletta [18] considering a constant heat flux boundary condition. The temperature field and the local Nusselt number were determined analytically by the Laplace transform method. Based on principles of first law of thermodynamics Nield and Lage [19] showed that, in case of slug flow, the value of the Nusselt number is not affected by finite axial conduction, either for uniform heat flux or isothermal boundary conditions. However, when the velocity varies along the transverse coordinate, the situation will be otherwise. Recently Haji-Sheikh et al. [20,21] solved the steady state conduction of heat from a wall to a fluid moving at a constant velocity by an integral transform technique. Although the problem appears to be a classical heat conduction problem, it is also valid for the slug flow heat transfer in an infinite tube/channel with a step change in wall temperature at the origin. Minkowycz and Haji-Sheikh [22] also studied a similar problem in both parallel-plate and circular ducts, and obtained asymptotic solutions for wall heat flux and bulk temperature near the thermal entrance location.

The slug flow problem is appropriate to a porous medium when Darcy's law is valid and also applicable for the hydrodynamically developing flow of a low Prandtl number fluid. The objectives of the present study are to investigate the two-dimensional forced convection for gaseous slip-flow in an infinite microtube with mixed boundary conditions. The velocity profile is assumed to be uniform along the radius of the tube. The energy equation has been solved by the method of separation of variables. Closed form solutions for bulk-mean temperature and Nusselt number are obtained in terms of Knudsen number, Peclet number and thermophysical properties of the fluid. The solution has been validated by comparing the results of fully-developed Nusselt numbers with those of macroscale case, by setting $Kn = 0$.

2. Mathematical model

In this study, the conventional slug flow problem in a circular tube is extended to include the microscale characteristics as well as the axial conduction effect. The analysis is based on steady, laminar, slug flow of an viscous fluid in an infinite circular tube subjected to mixed boundary conditions. The upstream part of the tube (from $Z = -\infty$ to $Z = 0$) is assumed to be insulated, while its downstream part (from $Z = 0$ to $Z = \infty$) is maintained at a constant temperature T_w (Fig. 1). The incompressible fluid with constant properties enters the tube at $Z = -\infty$, having a uniform temperature T_0. The heat flux at the wall surface is zero for $Z < 0$, and at the origin, there is a step change in heat flux due to convection for $Z > 0$. In the present analysis, the usual fluid continuum approach with temperature jump condition at the wall has been considered. The temperature jump is defined as [1]

$$T_s - T_w = -\frac{2 - F_t}{F_t}\frac{2\gamma}{\gamma + 1}\frac{\lambda}{Pr}\frac{\partial T}{\partial R}\bigg|_{R=R_0} \tag{1}$$

where T_s is temperature of the gas at the wall, T_w the wall temperature, λ the molecular mean free path, R_0 the radius of the tube, Pr the Prandtl number and F_t the thermal accommodation

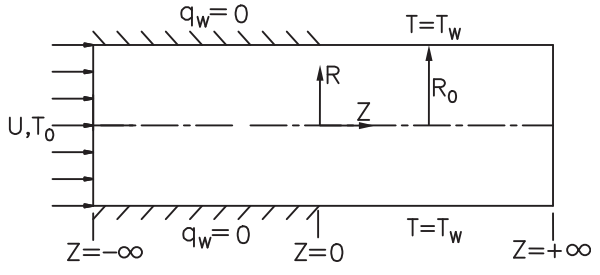

Fig. 1. Physical geometry of the infinite microtube.

coefficient, which depends on the fluid and surface material. Particularly for air, F_t assumes typical values near unity.

The steady-state energy equation for laminar flow in an infinite tube (Fig. 1) with uniform velocity distribution (without velocity jump) and neglecting the compressibility effect (assuming Mach number < 0.3) [23] can be written as

$$\rho c_p U\frac{\partial T}{\partial Z} = k\left[\frac{1}{R}\frac{\partial}{\partial R}\left(R\frac{\partial T}{\partial R}\right)+\frac{\partial^2 T}{\partial Z^2}\right] \quad 0<R<R_0, \quad -\infty<Z<\infty \tag{2}$$

Since the tube wall is maintained at a constant temperature T_w in the downstream part ($0<Z<\infty$), the fluid exchanges heat with the tube in this region and, at far downstream, the fluid attains the value of temperature T_w, equal to the wall temperature. Using the temperature jump condition at the wall (Eq. (1)) and utilizing the symmetry of temperature profiles about axis of the tube, the boundary conditions can be written as

$$T = T_w - \frac{4\gamma R_0}{\gamma+1}\frac{Kn}{Pr}\frac{\partial T}{\partial R} \quad \text{at } R=R_0, \quad 0<Z<\infty \tag{3a}$$

$$\frac{\partial T}{\partial R} = 0 \quad \text{at } R=R_0, \quad -\infty<Z<0 \tag{3b}$$

$$\frac{\partial T}{\partial R} = 0 \quad \text{at } R=0, \quad -\infty<Z<\infty \tag{3c}$$

$$T = T_0 \quad \text{at } Z\to-\infty \tag{3d}$$

$$T = T_w \quad \text{at } Z\to+\infty \tag{3e}$$

where, Kn is the Knudsen number. The energy equation (Eq. (2)) and the boundary conditions (Eq. (3)) are then made dimensionless by defining the following dimensionless variables:

$$r=\frac{R}{R_0}, \quad z=\frac{Z}{R_0}, \quad \theta=\frac{T-T_w}{T_0-T_w}, \quad Pe=\frac{\rho c_p U R_0}{k} \tag{4}$$

The energy equation after non-dimensionalization becomes

$$\frac{1}{r}\frac{\partial}{\partial r}\left(r\frac{\partial\theta}{\partial r}\right)+\frac{\partial^2\theta}{\partial z^2}-Pe\frac{\partial\theta}{\partial z}=0 \quad 0<r<1, \quad -\infty<z<\infty \tag{5}$$

The non-dimensional boundary conditions are

$$\left(\frac{4\gamma}{\gamma+1}\frac{Kn}{Pr}\right)\frac{\partial\theta}{\partial r}+\theta=0 \quad \text{at } r=1, \quad 0<z<\infty \tag{6a}$$

$$\frac{\partial\theta}{\partial r}=0 \quad \text{at } r=1, \quad -\infty<z<0 \tag{6b}$$

$$\frac{\partial\theta}{\partial r}=0 \quad \text{at } r=0, \quad -\infty<z<\infty \tag{6c}$$

$$\theta=1 \quad \text{at } z\to-\infty \tag{6d}$$

$$\theta=0 \quad \text{at } z\to+\infty \tag{6e}$$

In Eq. (6a), by setting $Kn\to 0$, the present formulation reduces to that of a conventional slug flow problem in an infinite tube. The objectives of the present work is to solve for the temperature field $\theta(r,z)$ and, to study the dependence of bulk-mean temperature $\theta_b(z)$ and Nusselt number $Nu(z)$ on Peclet number (Pe) and Knudsen number (Kn).

3. Analytical solution

The non-dimensional energy equation Eq. (5) and the associated boundary conditions in Eq. (6) have been solved by the method of separation of variables. For this purpose, the physical domain is divided into two regions: the isothermal zone A ($0<z<\infty$) and the adiabatic zone B ($-\infty<z<0$) and, with the cross section at $z=0$ as the dividing surface.

Separating the variables in Eq. (5) and using boundary conditions in Eqs. (6a), (6c) and (6e) lead to the following expression for the temperature distribution of the fluid in region A:

$$\theta_A(r,z) = \sum_{n=1}^{\infty} A_n J_0(\lambda_n r)\exp\left[-z\left(\sqrt{s^2+\lambda_n^2}-s\right)\right] \tag{7}$$

In the above equation, A_n are constants and the eigen values λ_n are positive roots of the following transcendental equation

$$J_0(\lambda)-\left(\frac{4\gamma}{\gamma+1}\frac{Kn}{Pr}\right)\lambda J_1(\lambda)=0 \tag{8}$$

and, J_0 and J_1 are Bessel functions of first kind of order zero and one respectively. Similarly, using boundary conditions in Eqs. (6b)–(6d), the temperature distribution of the fluid in the region B can be written as

$$\theta_B(r,z) = 1+\sum_{n=1}^{\infty} B_n J_0(\beta_n r)\exp\left[z\left(\sqrt{s^2+\beta_n^2}+s\right)\right] \tag{9}$$

where, B_n are constants and the eigen values β_n are positive roots of the following transcendental equation.

$$J_1(\beta)=0 \tag{10}$$

It may be noted that $\beta_1=0$ and $J_0(\beta_1 r)=1$. The coefficients A_n and B_n in Eqs. (7) and (9) are then determined by matching the compatibility conditions at the dividing surface between regions A and B. The compatibility conditions at the interface surface are continuity of the temperature and the axial heat flux:

$$\theta_A(r,0) = \theta_B(r,0) \tag{11a}$$

$$\left.\frac{\partial\theta_A}{\partial z}\right|_{z=0} = \left.\frac{\partial\theta_B}{\partial z}\right|_{z=0} \tag{11b}$$

Substituting Eqs. (7) and (9) in Eq. (11) yields

$$\sum_{n=1}^{\infty} A_n J_0(\lambda_n r) = 1+\sum_{n=1}^{\infty} B_n J_0(\beta_n r) \tag{12}$$

$$\sum_{n=1}^{\infty} A_n(-f_n) J_0(\lambda_n r) = \sum_{n=1}^{\infty} B_n g_n J_0(\beta_n r) \tag{13}$$

where, $f_n=\sqrt{s^2+\lambda_n^2}-s$ and $g_n=\sqrt{s^2+\beta_n^2}+s$. Now operating $\int_0^1 rJ_0(\beta_m r)\mathrm{d}r$, $m=1,2,\ldots$ on both sides of Eqs. (12) and (13), and by invoking the orthogonal properties of eigenfunctions, gives

$$\sum_{n=1}^{\infty} A_n\int_0^1 rJ_0(\lambda_n r)J_0(\beta_m r)\mathrm{d}r = \int_0^1 rJ_0(\beta_m r)\mathrm{d}r + B_m\int_0^1 rJ_0^2(\beta_m r)\mathrm{d}r \tag{14}$$

$$\sum_{n=1}^{\infty} A_n(-f_n)\int_0^1 rJ_0(\lambda_n r)J_0(\beta_m r)\mathrm{d}r = B_m g_m\int_0^1 rJ_0^2(\beta_m r)\mathrm{d}r \tag{15}$$

From Eq. (15), the value of B_m can be derived as

$$B_m = -\frac{\sum_{n=1}^{\infty} A_n f_n \int_0^1 r J_0(\lambda_n r) J_0(\beta_m r)\mathrm{d}r}{g_m \int_0^1 r J_0^2(\beta_m r)\mathrm{d}r} \tag{16}$$

Now substituting the value of B_m in Eq. (14) and rearranging the terms, leads to the following system of equations for the constants A_n:

$$\sum_{n=1}^{\infty} E_{mn} A_n = F_m, \quad m = 1,2,3,\ldots \tag{17}$$

where,

$$E_{mn} = \left(\sqrt{s^2+\lambda_n^2}+\sqrt{s^2+\beta_m^2}\right) \times \left[\frac{\lambda_n J_1(\lambda_n) J_0(\beta_m) - \beta_m J_1(\beta_m) J_0(\lambda_n)}{\lambda_n^2 - \beta_m^2}\right], \quad m = 1,2,3,\ldots \tag{18a}$$

$$F_m = \left(\sqrt{s^2+\beta_m^2}+s\right) \times \frac{J_1(\beta_m)}{\beta_m}, \quad m = 1,2,3,\ldots \tag{18b}$$

and, the limiting value of $J_1(\beta_1)/\beta_1$ in Eq. (18b) can be calculated using the L' Hospital's rule.

$$\underset{\beta_1 \to 0}{\text{Limit}} \frac{J_1(\beta_1)}{\beta_1} = 0.5 \tag{18c}$$

Equation (17) represents a system of infinite number of linear equations for the infinitely many unknowns A_n. As a common practice followed in all series solutions, numerical calculations are usually carried out by taking only a finite number of terms. So, in order to solve the system of equations (Eq. (17)) numerically, only a finite number of equations and terms, say $m = 1, 2,\ldots N$ and $n = 1, 2,\ldots N$ are considered. This leads to N linear equations with N unknowns $A_1, A_2, \ldots\ldots A_N$, which can be expressed as

$$[E]\{A\} = \{F\} \tag{19}$$

where, $[E]$ is a $N \times N$ matrix and, $\{A\}$ and $\{F\}$ are $N \times 1$ vectors. The numerical solutions for these simultaneous algebraic equations are obtained by an elimination method. After A_n have been solved, B_m are computed from Eq. (16):

$$B_m = -\frac{2\sum_{n=1}^{N} A_n \left(\sqrt{s^2+\lambda_n^2}-s\right)\left[\frac{\lambda_n J_1(\lambda_n) J_0(\beta_m) - \beta_m J_1(\beta_m) J_0(\lambda_n)}{\lambda_n^2 - \beta_m^2}\right]}{\left(\sqrt{s^2+\beta_m^2}+s\right)\left[J_0^2(\beta_m)+J_1^2(\beta_m)\right]} \tag{20}$$

It is worth to mention here that, since the eigenfunctions for regions A and B are both valid over the same fundamental domain $0 < r < 1$, it is also possible to obtain another set of equations similar to Eqs. (17) and (18) by operating Eqs. (12) and (13) with $\int_0^1 r J_0(\lambda_m r)\mathrm{d}r$. Although the resultant equations for E_{mn} and F_m so obtained are seemingly different from Eq. (19), the calculation reveals that both results are actually the same.

The following integrals involving Bessel function J_0 are adopted from Ref. [24] to evaluate A_n and B_m:

$$\int_0^1 r J_0(\lambda_n r) J_0(\beta_m r)\mathrm{d}r = \frac{[\lambda_n J_1(\lambda_n) J_0(\beta_m) - \beta_m J_1(\beta_m) J_0(\lambda_n)]}{\lambda_n^2 - \beta_m^2} \tag{21a}$$

$$\int_0^1 r J_0(\lambda_m r) J_0(\lambda_n r)\mathrm{d}r = \begin{cases} \dfrac{\left[J_0^2(\lambda_n)+J_1^2(\lambda_n)\right]}{2}, & \text{if } m = n \\ 0, & \text{if } m \neq n \end{cases} \tag{21b}$$

$$\int_0^1 r J_0(\lambda_m r)\mathrm{d}r = \frac{J_1(\lambda_m)}{\lambda_m} \tag{21c}$$

The local bulk-mean temperature $\theta_b(z)$ is calculated using the following expression:

$$\theta_b(z) = 2\int_0^1 \theta(r,z) r\,\mathrm{d}r \tag{22}$$

Utilizing Eqs. (7), (9) and (22), the local bulk-mean temperature is derived as

$$\theta_b(z) = \begin{cases} 2\sum_{n=1}^{N} \dfrac{A_n J_1(\lambda_n)}{\lambda_n} \exp\left[-z\left(\sqrt{s^2+\lambda_n^2}-s\right)\right] & \text{if } z \geq 0 \\ 1+2\sum_{n=1}^{N} \dfrac{B_n J_1(\beta_n)}{\beta_n} \exp\left[z\left(\sqrt{s^2+\beta_n^2}+s\right)\right] & \text{if } z \leq 0 \end{cases} \tag{23}$$

Finally the local Nusselt number $Nu(z)$, based on bulk-mean temperature, is calculated using the following expression:

$$Nu(z) = \frac{h(z) D_h}{k} = \frac{-2\frac{\partial\theta}{\partial r}\big|_{r=1}}{\theta_b} \tag{24}$$

Using Eqs. (7), (9), (23) and (24), the local Nusselt number has been deduced and given by

$$Nu(z) = \begin{cases} \dfrac{\sum_{n=1}^{N} A_n \lambda_n J_1(\lambda_n) \exp\left[-z\left(\sqrt{s^2+\lambda_n^2}-s\right)\right]}{\sum_{n=1}^{N} \dfrac{A_n J_1(\lambda_n)}{\lambda_n} \exp\left[-z\left(\sqrt{s^2+\lambda_n^2}-s\right)\right]} & \text{if } z > 0 \\ \dfrac{2\sum_{n=1}^{N} B_n \beta_n J_1(\beta_n) \exp\left[z\left(\sqrt{s^2+\beta_n^2}+s\right)\right]}{1+2\sum_{n=1}^{N} \dfrac{B_n J_1(\beta_n)}{\beta_n} \exp\left[z\left(\sqrt{s^2+\beta_n^2}+s\right)\right]} & \text{if } z < 0 \end{cases} \tag{25}$$

It may be verified that in Eq. (25), for the insulated wall ($z < 0$), $Nu(z) = 0$ since $J_1(\beta_n) = 0$, $n = 1,2,3, \ldots\ldots N$ from Eq. (10). Moreover, imposition of the continuity conditions of temperature and axial temperature gradient at the interface renders the bulk-mean temperature to be continuous at $z = 0$ in Eq. (23). Nevertheless, Nusselt number in Eq. (25) is still discontinuous at $z = 0$ because it involves normal temperature gradient.

4. Results and discussion

All calculations have been carried out with specific heat ratio $\gamma = 1.4$ and Prandtl number $Pr = 0.7$, which are the typical property

values of air. The values of Knudsen number Kn is varied between 0.001 and 0.1, which are the applicability limits of the slip-flow regime and Peclet number Pe is varied between 0.1 and 100. In the present formulation, the fluid temperature is so normalized that it varies from unity at inlet to zero at outlet. Hence the present analysis depicts the cooling of a hot fluid i.e. tube wall temperature is less than inlet temperature of the fluid and, accordingly, the results are interpreted. The eigen values λ_n and β_n in Eqs. (8) and (10) are estimated numerically using the Newton–Raphson method [25]. The first ten eigen values in Eq. (8) for different Knudsen numbers are tabulated in Table 1. The linear system of equations in Eq. (19) has been solved by the Gauss elimination method with equilibration, partial pivoting and iterative improvement [25]. Because of the step-change in normal temperature gradient $(\partial\theta/\partial r)$ at the triple interface $(z=0,\ r=1)$, the discontinuity of the surface heat flux causes a slow convergence of the series for small Knudsen numbers. In the present calculations, 600 terms in the series are found to be adequate to retain the accuracy of the solution. It can be shown from Eq. (25) that, for $z>0$, the fully-developed Nusselt number Nu_∞ is equal to λ_1^2. To check the correctness of the solution obtained herewith, calculations have also done for the macroscale case, by setting $Kn=0$. For $Kn=0$ with isothermal wall condition, $Nu_\infty=5.783$, which is the expected value found in literature [26].

The distribution of surface temperature of the fluid is shown in Fig. 2, for different Peclet numbers with $Kn=0.01$. It can be observed that the interface fluid temperature i.e. $\theta(1,0)$ as well as the temperature gradient at the interface $(\partial\theta(1,0)/\partial z)$ increase with increase in Peclet number. With constant fluid properties and fixed tube dimensions, Peclet number represents the fluid velocity. For the prescribed Kn number, $\theta(1,0)$ increases with increase in fluid velocity. This may be due to the fact that a higher velocity of the fluid allows less time for sufficient cooling to take place, resulting in a higher value of the interface temperature. The temperature gradient also increases with increase in Peclet number. This reveals the fact that at higher velocities, the axial conduction as well as axial convection across the interface may be significant. Fig. 3 shows the dependence of $\theta(1,0)$ on Knudsen number. Here, $\theta(1,0)$ increases with increase in Kn number for a given Pe. Since Knudsen number quantifies the extent of temperature jump at the surface, a higher Knudsen number means less heat transfer to the cold wall in the downstream. This reduced heat transfer may cause to increase $\theta(1,0)$. The above trends are in obvious accord with what one would expect on a physical ground: $\theta(1,0)$ always increases as Knudsen number increases, reflecting the fact that heat transfer from the fluid is decreased.

The axial variation of bulk-mean temperature $\theta_b(z)$ is demonstrated in Fig. 4 for different Pe numbers and in Fig. 5 for different Kn numbers. In both the cases, θ_b has a value of unity at the tube inlet and monotonically decreases longitudinally along the tube. Beyond the entrance region, the value of θ_b approaches to zero as

Table 1
First ten eigen values of Eq. (8) with $Pr=0.7$ and $\gamma=1.4$.

First ten eigen values of Eq. (8) with $Pr=0.7$ and $\gamma=1.4$						
$\lambda\backslash Kn$	0	0.001	0.005	0.01	0.05	0.1
λ_1	2.40483	2.39682	2.3651	2.32614	2.04901	1.78866
λ_2	5.52008	5.50171	5.42909	5.34098	4.80331	4.46337
λ_3	8.65373	8.62494	8.51164	8.37707	7.70389	7.41027
λ_4	11.79153	11.75231	11.59901	11.42215	10.69639	10.4566
λ_5	14.93092	14.88127	14.68889	14.4748	13.74138	13.54344
λ_6	18.07106	18.011	17.78068	17.53481	16.81676	16.64985
λ_7	21.21164	21.14117	20.87423	20.60204	19.91067	19.76705
λ_8	24.35247	24.27161	23.96952	23.6762	23.01649	22.89077
λ_9	27.49348	27.40224	27.06657	26.75684	26.13034	26.01872
λ_{10}	30.63461	30.53301	30.1654	29.84346	29.24985	29.14957

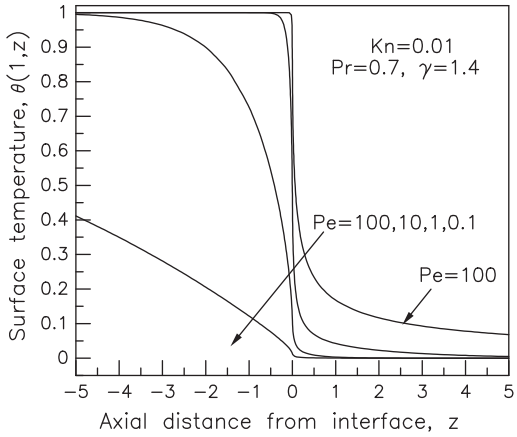

Fig. 2. Surface temperature distribution at the interface for different Peclet numbers with $Kn=0.01$.

the fluid temperature attains the wall temperature at this location. The dependence of bulk-mean temperature at the interface on Pe and Kn are shown in Table 2 and plotted in Fig. 6, and it can be observed that $\theta_b(0)$ always increases with increase in Pe number or increase in Kn number.

In Fig. 7, the effect of Pe on local Nusselt number is demonstrated for macrochannels with $Kn=0$. The curves for the different Pe numbers eventually merge together and approach the asymptotic fully-developed value of 5.783. It may also be observed that, in the entrance region, Nu number increases with increase in Pe, which substantiates the fact that Reynolds analogy holds good in this region. Besides, the thermal entrance length increases with increase in Pe number. The above results are in qualitative agreement with the Bejan's conjecture [26, pp. 97] based on scale analysis:

$$Nu(z)=\frac{hD_h}{k}\propto\left(\frac{z}{Pe}\right)^{-0.5} \tag{26}$$

which is valid for both laminar slug flow and Hagen–Poiseuille flow in the thermally developing region. The variation of local Nusselt number for $Kn=0.01$ is shown in Fig. 8. In this case, although the nature of the graph is similar to those shown in Fig. 7, the fully-developed Nusselt number attains the asymptotic value of 5.411 for all values of Pe. A similar trend of results is also reported by Jeong and Jeong [2,12] for slip-flow heat transfer in a channel with parabolic velocity profile. In both Figs. 7 and 8, the local Nu number

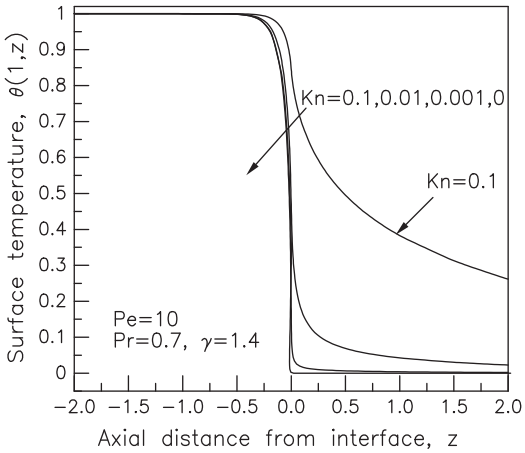

Fig. 3. Surface temperature distribution at the interface for different Knudsen numbers with $Pe=10$.

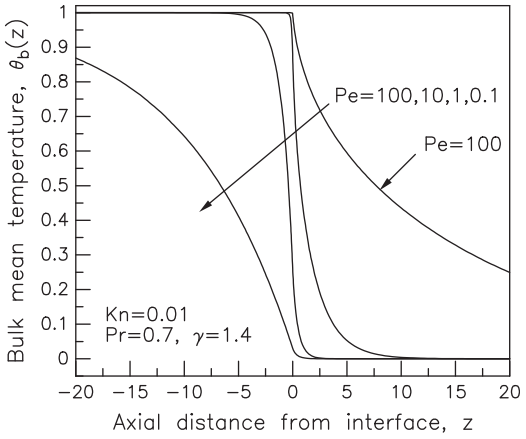

Fig. 4. Axial variation of bulk-mean temperature for different Peclet numbers with $Kn = 0.01$.

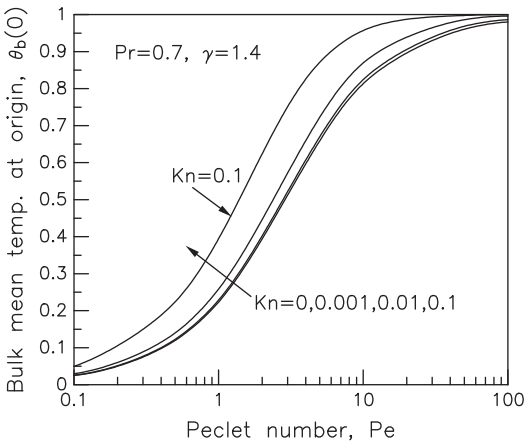

Fig. 6. Variation of bulk-mean temperature at the origin $\theta_b(0)$ with Peclet and Knudsen numbers.

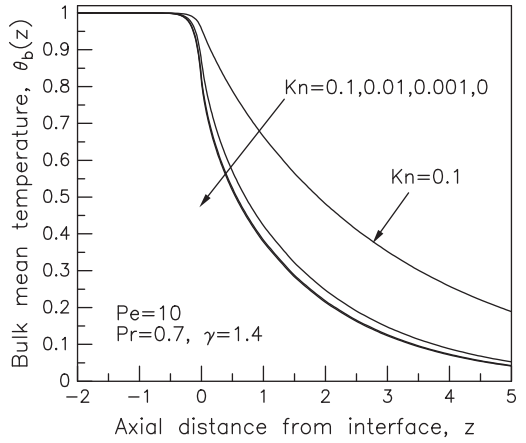

Fig. 5. Axial variation of bulk-mean temperature for different Knudsen numbers with $Pe = 10$.

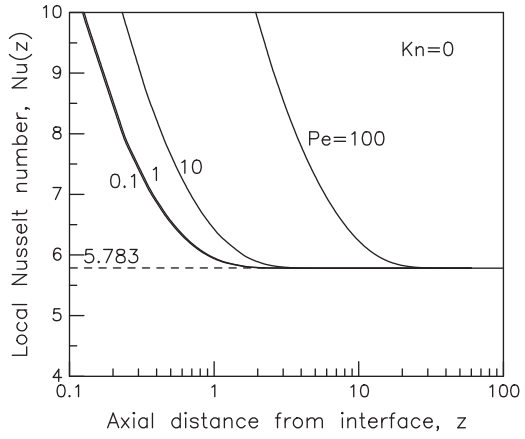

Fig. 7. Axial variation of local Nusselt number for different Peclet numbers with $Kn = 0$.

tends to reach infinity at the origin ($z = 0$) for all *Pe* numbers. This is because, the thermal boundary layer thickness is zero at $z = 0$ and thereby the temperature gradient at the wall is infinite at this location. However, *Nu* decays rapidly as the thermal boundary layer develops, until the constant value associated with fully-developed condition is reached.

Fig. 9 shows the effects of rarefaction, represented by *Kn*, on the local Nusselt number along the tube. As discussed above it can be realized that Nusselt numbers are, in principle, infinite at $z = 0$ and decays to their asymptotic (fully-developed) values Nu_∞ with increasing *z*. It is seen that Nusselt number, the representative of heat transfer, always decreases with increase in *Kn* and this trend is in agreement with results reported in [7,11,12]. These results may be explained by noting that, as the flow departs from the continuum behavior, a reduction in heat transfer at the surface occurs because the temperature gradient at the surface becomes smaller due to the temperature jump. Therefore, as *Kn* increases, the temperature gradient at the wall decreases and the decreased temperature gradient reduces the heat transfer. Finally, in Fig. 10, the fully-developed Nusselt numbers are illustrated graphically against

Table 2
Bulk-mean temperature at the origin, $\theta_b(0)$.

Bulk-mean temperature at the origin, $\theta_b(0)$				
*Pe**Kn*	0	0.001	0.01	0.1
0.1	0.0252	0.0259	0.0297	0.0496
1.0	0.2236	0.2289	0.2586	0.3946
10.0	0.8136	0.8243	0.8696	0.9572
100.0	0.9803	0.9863	0.9956	0.9994

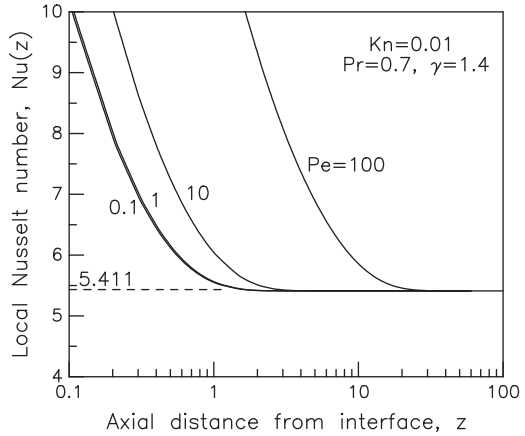

Fig. 8. Axial variation of local Nusselt number for different Peclet numbers with $Kn = 0.01$.

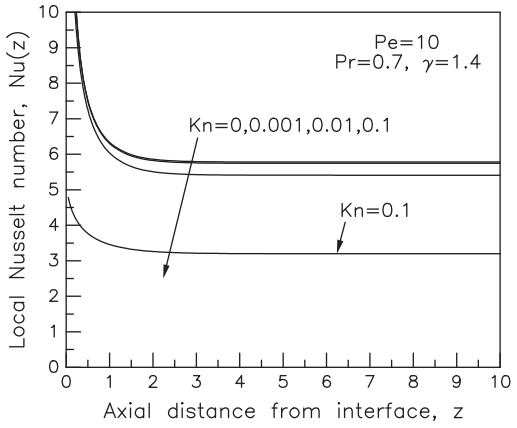

Fig. 9. Axial variation of local Nusselt number for different Knudsen numbers with $Pe = 10$.

various Knudsen numbers. For thermally fully-developed flow, both numerator and denominator of Eq. (24) tend to zero, leading to a finite value of the Nusselt number. It is observed that the fully-developed Nusselt number decreases with increase in *Kn* number, which are in consistence with Fig. 9. In Fig. 10, the present solution has been compared with solutions available for Poiseuille flow without viscous dissipation [11,12]. At $Kn = 0$, the value of Nu_∞ is 5.783 for slug flow, while for Poiseuille flow $Nu_\infty = 3.675$. However, as *Kn* number increases, the Poiseuille profiles become increasingly flat and, thereby, the difference of Nu_∞ values gradually decreases.

Reported literature [27] indicates that, for heat sink applications, the temperature range normally considered is 20 °C to 70 °C. Considering air as the coolant, the variation of thermophysical properties (at atmospheric pressure) from channel inlet to exit are: Prandtl number: 1% (decrease) and thermal diffusivity: 33% (increase). Although the variation of *Pr* is marginal, the variation of thermal diffusivity (associated with *Pe*) may not be overlooked, for which temperature dependent thermal properties need to be considered in the model. The solution of mixed boundary value problems by the classical method of separation of variables may not be convenient since the boundary conditions involve discontinuities. The discontinuity of the surface heat flux at the interface increases with decease in Knudsen number and results in slow convergence of the series, which is inherent in a separation of variables solution. Due to this reason, specialized integral transform methods such as Wiener–Hopf technique [28] may be useful for solving these problems.

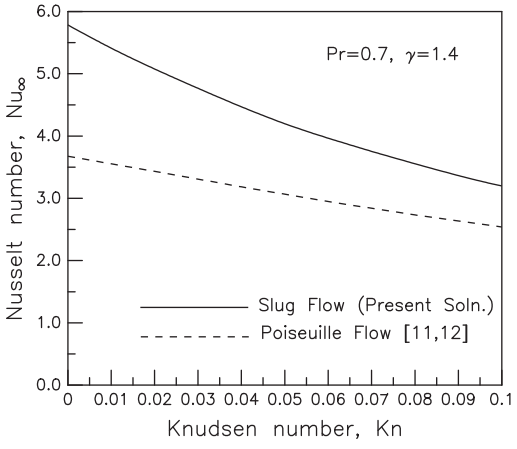

Fig. 10. Variation of fully developed Nusselt number Nu_∞ with Knudsen number with $Pr = 0.7$ and $\gamma = 1.4$.

5. Conclusion

In this study, the conventional slug flow problem in an infinite tube is extended to include both slip-flow characteristics and axial conduction effect. The energy equation is solved analytically by the separation of variables method and, closed form solutions for bulk-mean temperature and Nusselt number are derived in terms of Peclet number and Knudsen number. It is concluded that:

- For the hot fluid and cold wall situation, in the thermal entrance region, the local bulk-mean temperature increases as Peclet number or Knudsen number increases. Also, the thermal entrance length increases as Peclet number or Knudsen number increases. The results will be opposite if the flow situation is reversed.
- In the thermal entrance region, the local Nusselt number increases with increase in Peclet number but decreases with increase in Knudsen number. The fully-developed Nusselt number decreases with increase in Knudsen number but, for a fixed value of Knudsen number, it reaches a constant value for all Peclet numbers.

Acknowledgments

The financial support from Grant No. F.26-14/2003, TSV, Dt. 14.01.04, MHRD, is gratefully acknowledged.

References

[1] G.E. Karniadakis, A. Beskok, Micro Flows, Fundamentals and Simulation, Springer, New York, 2002.
[2] H.E. Jeong, J.T. Jeong, Extended Graetz problem including streamwise conduction and viscous dissipation in microchannel, Int. J. Heat Mass Transfer 49 (2006) 2151–2157.
[3] N.G. Hadjiconstantinou, O. Simek, Constant-wall-temperature Nusselt number in micro and nano-channels, ASME J. Heat Transfer 124 (2002) 356–364.
[4] S.P. Yu, T.A. Ameel, Slip-flow heat transfer in rectangular microchannels, Int. J. Heat Mass Transfer 44 (2001) 4225–4235.
[5] G. Tunc, Y. Bayazitoglu, Heat transfer in rectangular microchannels, Int. J. Heat Mass Transfer 45 (2002) 765–773.
[6] C.H. Chen, Slip-flow heat transfer in a microchannel with viscous dissipation, Heat Mass Transfer 42 (2006) 853–860.
[7] O. Aydin, M. Avci, Analysis of laminar heat transfer in micro-Poiseuille flow, Int. J. Thermal Sci. 46 (2007) 30–37.
[8] R.F. Barron, X.M. Wang, R.O. Warrington, T.A. Ameel, The Graetz problem extended to slip flow, Int. J. Heat Mass Transfer 40 (1997) 1817–1823.
[9] T.A. Ameel, R.F. Barron, X.M. Wang, R.O. Warrington, Laminar forced convection in a circular tube with constant heat flux and slip flow, Microscale Thermophys. Eng. 1 (1997) 303–320.
[10] F.E. Larrode, C. Housiadas, Y. Drossinos, Slip flow heat transfer in circular tubes, Int. J. Heat Mass Transfer 43 (2000) 2669–2680.
[11] G. Tunc, Y. Bayazitoglu, Heat transfer in microtubes with viscous dissipation, Int. J. Heat Mass Transfer 44 (2001) 2395–2403.
[12] H.E. Jeong, J.T. Jeong, Extended Graetz problem including axial conduction and viscous dissipation in microtube, J. Mech. Sci. Tech. 20 (2006) 158–166.
[13] O. Aydin, M. Avci, Heat and fluid flow characteristics of gases in micropipes, Int. J. Heat Mass Transfer 49 (2006) 1723–1730.
[14] O. Aydin, M. Avci, Analysis of micro-Graetz problem in a microtube, Nanoscale Microscale Thermophys. Eng. 10 (2006) 345–358.
[15] S. Golos, Theoretical investigation of the thermal Entrance region in steady, axially symmetrical slug flow with mixed boundary conditions, Int. J. Heat Mass Transfer 13 (1970) 1715–1725.
[16] V.P. Tyagi, K.M. Nigam, On closed-form analytical solution for circular duct thermally developing slug flow under mixed boundary condition, Int. J. Heat Mass Transfer 18 (1975) 1253–1256.
[17] A. Barletta, E. Zanchini, Forced convection in the thermal entrance region of a circular duct with slug flow and viscous dissipation, Int. J. Heat Mass Transfer 40 (1997) 1181–1190.
[18] A. Barletta, Slug flow heat transfer in circular ducts with viscous dissipation and convective boundary conditions, Int. J. Heat Mass Transfer 40 (1997) 4219–4228.
[19] D.A. Nield, J.L. Lage, The role of longitudinal diffusion in fully developed forced convective slug flow in a channel, Int. J. Heat Mass Transfer 30 (1998) 3264–3266.
[20] A. Haji-Sheikh, D.E. Amos, J.V. Beck, Axial heat conduction in a moving semi-infinite fluid, Int. J. Heat Mass Transfer 51 (2008) 4651–4658.

[21] A. Haji-Sheikh, D.E. Amos, J.V. Beck, Temperature field in a moving semi-infinite region with a prescribed wall heat flux, Int. J. Heat Mass Transfer 52 (2009) 2092–2101.
[22] W.J. Minkowycz, A. Haji-Sheikh, Asymptotic behaviors of heat transfer in porous passages with axial conduction, Int. J. Heat Mass Transfer 52 (2009) 3101–3108.
[23] G.L. Morini, M. Lorenzini, M. Spiga, A criterion for experimental validation of slip-flow models for incompressible rarefied gases through microchannels, Microfluid Nanofluid 1 (2005) 190–196.
[24] F. Bowman, Introduction to Bessel functions, Dover Publications, New York, 1958.
[25] W.H. Press, S.A. Teukolsky, W.T. Vetterling, B.P. Flannery, Numerical Recipes in FORTRAN, Cambridge University Press, 1998.
[26] A. Bejan, Convection Heat Transfer, Wiley-Interscience, New York, 1984.
[27] Z. Li, X. Huai, Y. Tao, H. Chen, Effects of thermal property variations on the liquid flow and heat transfer in microchannel heat sinks, Appl. Thermal Eng. 27 (2007) 2803–2814.
[28] J.S. Vrentas, C.M. Vrentas, Axial conduction with boundary conditions of the mixed type, Chem. Eng. Sci. 62 (2007) 3104–3111.